

# Scalable testing of quantum error correction

John Zhuoyang Ye and Jens Palsberg

University of California, Los Angeles

The standard method for benchmarking quantum error-correction is randomized fault-injection testing. The state-of-the-art tool Stim is efficient for error correction implementations with distances of up to 10, but scales poorly to larger distances for low physical error rates. In this paper, we present a scalable approach that combines stratified fault injection with extrapolation. Our insight is that some of the fault space can be sampled efficiently, after which extrapolation is sufficient to complete the testing task. As a result, our tool scales to distance 17 for a physical error rate of 0.0005 with a two-hour time budget on a desktop. For this case, it estimated a logical error rate of  $1.51 \times 10^{-11}$  with high confidence.

## Contents

<b>1</b>	<b>Introduction</b>	<b>1</b>
<b>2</b>	<b>Examples of How Stim Works</b>	<b>2</b>
2.1	Distance and Logical Error Rate . . . . .	2
2.2	Repetition Code . . . . .	2
2.3	Surface Code . . . . .	3
<b>3</b>	<b>Modeling QEC-Test Data</b>	<b>4</b>
<b>4</b>	<b>Separating Low and High Weights</b>	<b>7</b>
<b>5</b>	<b>Testing Samples with High Weights</b>	<b>7</b>
5.1	Our Approach . . . . .	8
5.2	Example . . . . .	8
<b>6</b>	<b>Our Algorithm</b>	<b>10</b>
6.1	Pseudo-code for Our Algorithm . . . . .	10
6.2	Example . . . . .	10
<b>7</b>	<b>Implementation</b>	<b>10</b>
<b>8</b>	<b>Evaluation</b>	<b>11</b>
8.1	RQ1: Scalability Comparison . . . . .	11

8.2	RQ2: Agreement Check . . . . .	13
8.3	RQ3: S-curve Comparison . . . . .	15
<b>9</b>	<b>Threats to Validity</b>	<b>15</b>
<b>10</b>	<b>Related Work</b>	<b>16</b>
<b>11</b>	<b>Future Work</b>	<b>17</b>
<b>12</b>	<b>Conclusion</b>	<b>17</b>
	<b>References</b>	<b>18</b>

## 1 Introduction

**Background.** Quantum computing has made rapid progress this decade, including a breakthrough in 2024 when researchers demonstrated that *quantum error correction (QEC)* [1, 2, 3] can partially suppress quantum-hardware errors [4]. This breakthrough paves the way for fault-tolerant quantum computing, which is expected to become a reality in the next decade and begin to have an impact on science and business [5, 6, 7].

Experimental papers on QEC often express the quality of their approaches by stating the *logical error rate*, which is the probability that a program execution gives a wrong result [8]. Typically, such papers estimate the logical error rate through *testing* of the quantum circuit that implements the QEC algorithm [9, 10, 11]. Most of these circuits are too large for current quantum computers, so instead the authors simulate them on classical computers, using a model of quantum-hardware errors [12]. Thus, the benchmarking challenge boils down to a testing campaign on a classical computer with the goal of estimating the logical error rate with high confidence.

For high-quality QEC algorithms with low logical error rates, the testing required is massive and has become a major obstacle for researchers [13, 14, 9, 15, 16]. Furthermore, the lower the

logical error rate, the more testing is needed to estimate what it is [17, 18, 19]. The goal of this paper is to greatly reduce the testing effort for high-quality QEC algorithms.

**State of the Art.** Gidney’s popular tool Stim [13] uses randomized fault injection testing [20] to benchmark an implementation of quantum error correction. Stim repeatedly injects random faults into a circuit and checks for logical errors. However, for high-quality QEC algorithms, logical errors are rare events, forcing Stim to run a massive number of tests to achieve statistical confidence. For example, for a surface code with distance 13 and for a physical error rate of 0.0005, Stim found no logical errors at all after running for two hours on a desktop. This motivated us to design a more scalable approach.

**Our Results.** We present ScaLER (Scalable Logical Error Rate Testing), an efficient and scalable approach to benchmarking implementations of quantum error correction. Our insight is that some of the fault space can be sampled efficiently, after which extrapolation is sufficient to complete the testing task. For example, for a surface code with distance 17 and for a physical error rate of 0.0005, ScaLER estimated the logical error rate with high confidence after running for two hours on a desktop. For this time budget, ScaLER estimated a logical error rate of  $1.51 \times 10^{-11}$ . In contrast, for the same time budget, the lowest logical error rate that Stim estimated with high confidence was  $5.95 \times 10^{-6}$  for a surface code with distance 7.

**The Rest of the Paper.** In Section 2, we give examples of how Stim works, in Section 3, we discuss how to model QEC-test data, and in Sections 4–6, we present our algorithm. In Section 7, we present our implementation, in Section 8, we detail the evaluation of our approach, and in Section 9, we discuss threats to validity. Finally, in Sections 10–11 we discuss related and future work, and in Section 12, we conclude.

Our software is publicly available under an open-source license at this link:

<https://github.com/yezhuoyang/ScaLERQEC>.

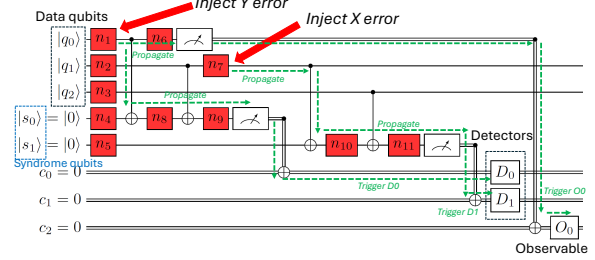


Figure 1: Diagram for injecting SID error model to a  $[[3, 1, 3]]$  repetition code circuit which protect logical  $|0\rangle$  state. There are 11 error locations indexed by  $n_i$ ,  $i \in [1, 11]$ . We inject fault  $n_7 = X$ , which will trigger detector  $D_1 = 1$  after propagation. We also inject fault  $n_1 = Y$ , which trigger detector  $D_0 = 1$  and also flip observable result  $O_0 = 1$ .

## 2 Examples of How Stim Works

In this section, we recall the relationship between distance and logical error rate, and we discuss how Stim works and why it scales poorly. Our examples are a repetition code with distance 3 and a surface code with distance 7.

### 2.1 Distance and Logical Error Rate

For QEC implementations, a higher distance means a lower logical error rate. In other words, larger scale means better quality. Medium-scale distances are 5–13, while large-scale distances range from 15 and up, with 27 as a particularly well-studied point [21]. A QEC algorithm with distance  $d$  can correct  $(d - 1)/2$  errors, so higher is better, but what if more than  $(d - 1)/2$  errors occur? In some cases, a QEC algorithm successfully handles such cases, while in others, the results are logical errors. Researchers summarize a testing campaign by estimating the logical error rate as the number of logical errors divided by the number of tests.

### 2.2 Repetition Code

Let us see how Stim estimates the logical error rate for the circuit in Figure 1, which implements a repetition code with distance 3. Specifically, it encodes a source-level qubit as three data qubits  $|q_0\rangle, |q_1\rangle, |q_2\rangle$ , uses two detectors  $D_0, D_1 \in \{0, 1\}$  for mid-circuit error detection, and lets  $O_0 \in \{0, 1\}$  denote the result of measuring the encoded qubit. Stim models quantum-hardware errors by repeatedly injecting faults into the circuit and

Index	Error	$D_0$	$D_1$	$O_0$	Decoder output	Predicted $O_0$	Logical error?
1	$n_1 = X$	1	0	1	$n_4 = X$	0 ( $\neq 1$ )	Yes
2	$n_2 = X$	1	1	0	$n_2 = X$	0	No
3	$n_3 = X$	0	1	0	$n_3 = X$	0	No
4	$n_4 = X$	1	0	0	$n_4 = X$	0	No
5	$n_5 = X$	0	1	0	$n_3 = X$	0	No
6	$n_6 = X$	0	0	1	No Error	0 ( $\neq 1$ )	Yes
7	$n_7 = X$	0	1	0	$n_3 = X$	0	No
8	$n_8 = X$	1	0	0	$n_4 = X$	0	No
9	$n_9 = X$	1	0	0	$n_4 = X$	0	No
10	$n_{10} = X$	0	1	0	$n_3 = X$	0	No
11	$n_{11} = X$	0	1	0	$n_3 = X$	0	No

Table 1: All 11 cases with one Pauli X error when the logical state is 0. The outcomes of the detector/observable are calculated by tracking the propagation of the injected error.

then testing whether the circuit still works correctly. Conceptually, Stim does that by:

1. picking a random list of circuit locations,
2. injecting an X-gate, Y-gate, or Z-gate into each of those locations, and
3. testing whether the modified circuit works correctly, with the help of a decoder.

We will refer to the modified circuit as a *sample*. If the list of locations has length  $w$ , then we say that the sample has weight  $w$ . Our example circuit in Figure 1 has 11 locations in which Stim can inject faults. Here, we restrict the noise model to Pauli- $X$  errors only, ignoring  $Y$  and  $Z$  errors. Table 1 summarizes a testing campaign with 11 samples, all with weight 1. Stim found that 2 of the 11 samples give a logical error, while the rest work correctly. From this testing campaign, our estimate of the logical error rate  $P_L$  is:

$$P_L \approx \frac{\text{number of logical errors}}{\text{number of samples}} = \frac{2}{11} \quad (1)$$

### 2.3 Surface Code

Let us see why Stim scales poorly. We added lightweight logging hooks to Stim to record the Pauli-weight for every sample. Figure 2 summarizes the testing campaign of Stim for a surface code with distance 7, showing, for each weight, the number of samples and the number of logical errors. The low-weight samples dominate, which is due to the error model that we use. Our model is a variant of a popular error model called SD6 [23, 9]. We call our model SID, which is short for the *uniform single-qubit circuit-level independent depolarizing noise model*. This model has

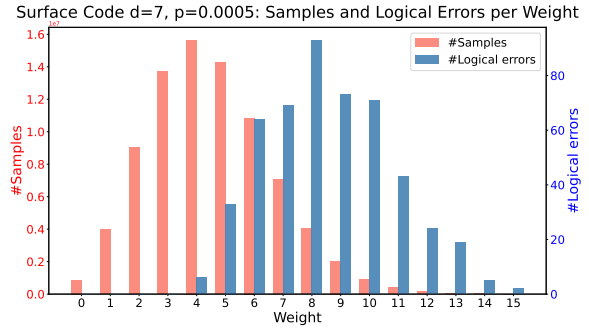


Figure 2: We run Stim on Surface code with distance 7 and physical error rate  $5 \times 10^{-4}$  and plot the number of samples (red bars) and the number of logical errors (blue bars) for each weight. Below  $w = 3$ , the circuit is fault-tolerant and Stim cannot sample any logical errors. Beverland et al. and Carolyn Mayer et al. report similar observations in their recent papers [22, 22].

a single parameter  $p$ , known as the *physical error rate*, which is the probability that a gate, a measurement, or an idling step works incorrectly due to depolarization noise. The model assumes that such errors are independent of each other and that each error can be modeled by injecting an X-gate, Y-gate, or Z-gate. This implies that the model excludes correlated Pauli errors [24].

*We use the SID model with  $p = 0.0005$ , unless noted explicitly.*

This models some of the best quantum-hardware today, taking into account circuit-level behavior such as measurement/reset error and hook errors [1, 8, 25]. In addition,  $p = 0.0005$  is better than the threshold required for quantum error correction to be successful. In Section 8, we experiment with  $p$  down to  $p = 0.0001$  to stress test our method.

In the SID error model, Stim uses  $p$  to determine a weighted binomial distribution (Figure 2) centered on  $p$  multiplied by the number of locations in the circuit. The circuit for the surface code with distance 7 has 9,121 locations, so Stim centers the weight distribution around  $0.0005 \times 9,121 \approx 4$ . In total, Stim tried 83,000,000 samples and found 503 logical errors, from which we can estimate the logical error rate:

$$P_L \approx \frac{\text{number of logical errors}}{\text{number of samples}} = \frac{503}{83,000,000} = 6.06 \times 10^{-6}$$

Figure 2 shows that the proportion of logical errors sampled is low at low weights, but higher at higher weights. This crystallizes the reason why Stim scales poorly: it tests mostly low-weight samples, which have few logical errors. Indeed, for our example, Stim spent 8.22 minutes on low-weight samples (weights 0–8) but only 0.37 minutes on high-weight samples (weights 9–15). When the distance increases, the threshold theorem [26, 27] says that the logical error rate decreases exponentially. Our experiments with Stim confirm this: when we increased the distance of the surface code from 7 to 13, the number of logical errors decreased from 503 to 0. If we were to use this outcome to estimate the logical error rate, we would get 0, which is wrong.

In this paper, we do the opposite of Stim: we test only high-weight samples and use the results to predict the results for low-weight samples. This scales well because high-weight samples readily produce logical errors and because we have an efficient prediction method.

### 3 Modeling QEC-Test Data

In this section, we show how to model the data from any QEC-testing campaign. Such a model enables us to use the results for high-weight samples to predict the results for low-weight samples.

**Stratified Logical Error Rates.** Our first step is to reformulate the definition in Equation 1 of how to estimate the logical error rate from the QEC-test data, as in Figure 2. For each weight  $w$ , we can calculate the logical error rate  $P_L^w$  for that  $w$ , as shown in Equation 2. This enables us to sum up those probabilities  $P_L^w$ , weighted by the probability that  $w$  faults occur, as shown in Equation 3.

$$\begin{aligned} P_L^w &= P(\text{logical error at weight } w) \\ &\approx \frac{\# \text{ logical errors at weight } w}{\# \text{ samples at weight } w} \end{aligned} \quad (2)$$

$$\begin{aligned} P_L &= P(\text{logical error}) \\ &\approx \sum_w P_L^w \times P(w \text{ faults occur}) \end{aligned} \quad (3)$$

For a physical error rate  $p$  and a circuit with  $C$  locations, we have:

$$P(w \text{ faults occur}) = \binom{C}{w} p^w (1-p)^{C-w} \quad (4)$$

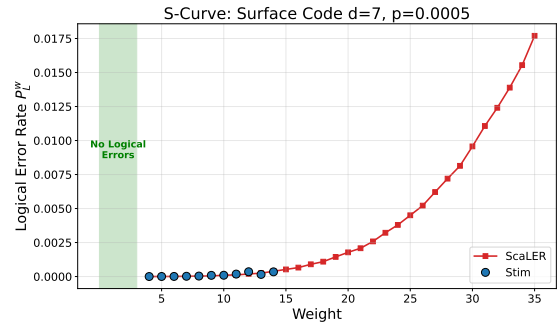


Figure 3: S-curve data (Surface code  $d=7$ ,  $p = 5 \times 10^{-4}$ ) combining Stim samples and ScaLER extensions.

Equation 4 is correct for the error model we use because for a weight  $w$ , there are  $3^w \binom{C}{w}$  different error configurations that each occur with probability  $(\frac{p}{3})^w (1-p)^{C-w}$ . Notice that  $3^w$  and  $(\frac{1}{3})^w$  cancel each other out.

**The Logical Error Rates Form an S-Curve.** For the data in Figure 2, we can plot  $P_L^w$  as a function of  $w$ , which produces the blue data points in Figure 3. In the left part of Figure 3, for low weights, we have the fault-tolerant zone where the logical error rate is 0. This zone goes from weight 0 to  $(d-1)/2 = 3$ . From weights 4 to 14, we have blue  $P_L^w$  data points based on Figure 2 and Equation 2, and from weights 15 to 35 we have red  $P_L^w$  data points that we calculated after using our own tool ScaLER to perform random tests for these weights.

In Figure 3, the red data points show a steep rise, which can make us wonder what happens for weights higher than 35. We answer this by continuing the random testing for weights greater than 35, see Figure 4. The data forms an S-curve that flattens out at 0.5, which is where the physical errors saturate the circuit and the logical errors happen with probability 0.5, like a coin flip. We tried this experiment with also a toric code and a BB code [28], and we tried for different distances. The results are shown in Figure 4. In every case, we see a curve shaped as the letter S, which leads us to call them S-curves. We tried other cases beyond those shown in Figure 4 and in every case we saw an S-curve.

We want to model the S-curves that emerge from the QEC-test data. For our purposes, the best kind of model is a continuous function. We will use  $\mathbb{R}^+$  to denote the set of nonnegative real numbers.

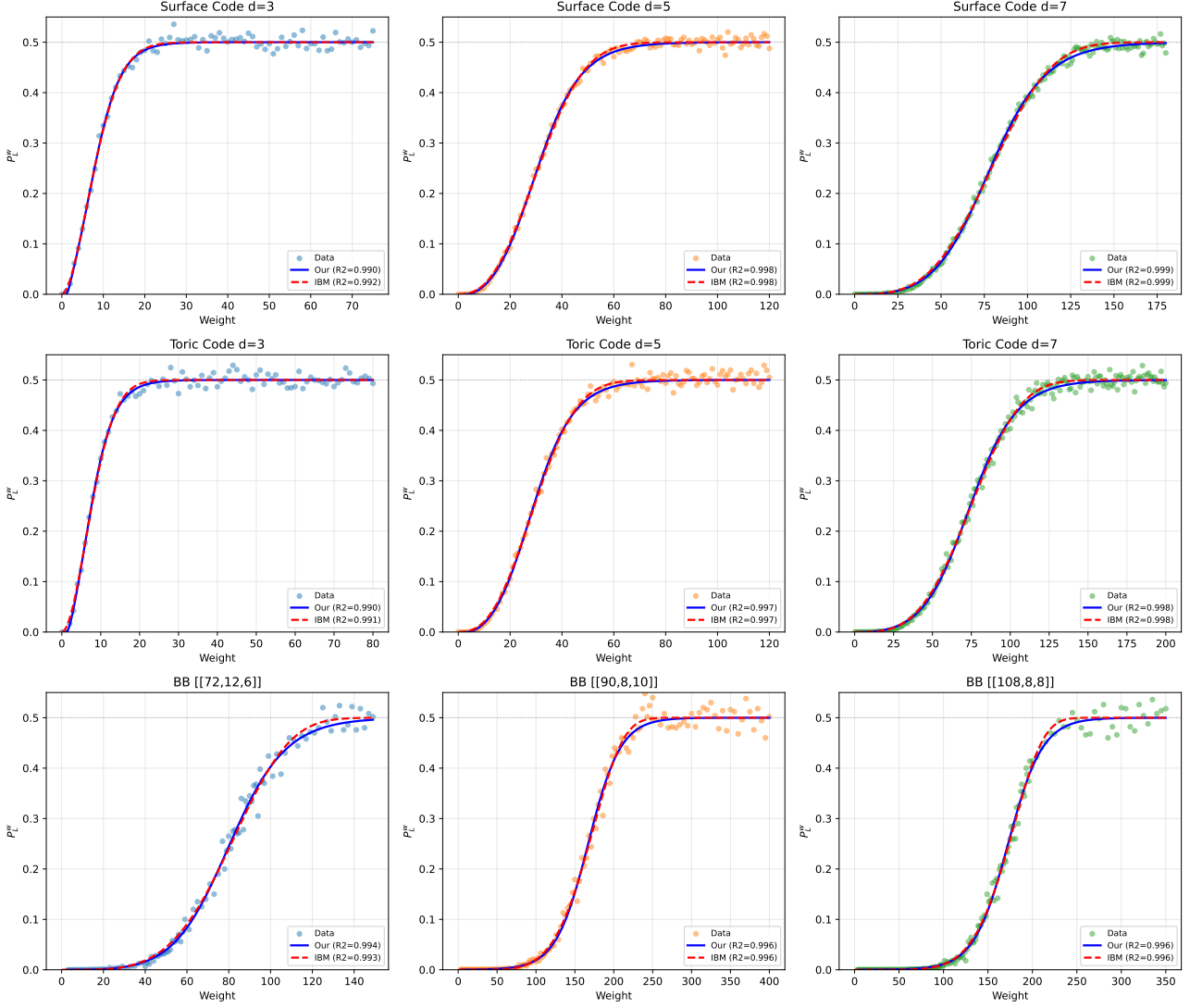


Figure 4: We fit the data collected by small scale QEC circuit ( $d=3,5,7$ ) for Surface code, Toric code and Bivariate Bicycle code by both S-curve model under single qubit depolarization noise model and . Both models fits perfectly well with the observed data for all three codes. We calculate the  $R^2$  score to evaluate the curve fitting.  $R^2 > 0.99$  for all cases(Table 2).

**Definition 1** (Modeling S-Curves). *We have the following requirements for a function  $f$  that models the S-curve in QEC-test data:*

- $f : \mathbb{R}^+ \rightarrow \mathbb{R}^+$  and is twice differentiable (except at 0).
- $f(0) = 0$ .
- $f$  is increasing.
- $\lim_{w \rightarrow \infty} f(w) = 0.5$ .
- $f''$  changes sign from + to - at an inflection point.

Previous work in many fields has defined functions that satisfy the requirements in Definition 1, particularly for purposes such as neural-network training [29, 30], natural-phenomena modeling [31, 32, 33], and prediction of software-failure [34, 35]. Now we give a couple of specific definitions of  $f$  that satisfy those requirements, and then we show that they fit the QEC-test data well. First, we consider one of the recently proposed ansatz S-curve models as an illustrative example.

**Definition 2** (IBM's S-Curve Model). *The seminal paper by Beverland et al. [19] from IBM defined the following ansatz function with three pa-*

rameters to learn, called the *Min-Fail Enclosure Model*. The function takes as input an integer  $w \geq 0$ :

$$f_t^{IBM}[\mu, \alpha, \beta](w) = \frac{1}{2} \left[ 1 - \exp\left(-2\mu \left(\frac{w}{\beta}\right)^\alpha\right) \right] \quad (5)$$

In the paper [19],  $\beta$  denotes the smallest error weight that triggers a logical error, called the *onset* weight. One can easily check that  $f_t^{IBM}[\mu, \alpha, \beta]$  satisfies the requirements in Definition 1.

In IBM's S-curve model, the onset weight ( $\beta$  in Equation 5) is a parameter to fit or to be found through a computationally intensive and unscalable search. This led us to treat  $\beta$  as a parameter to fit. (We did try hard-coding  $\beta = t+1$ , but this fits the QEC-data poorly.)

We assume that we know the distance  $d$  of the QEC circuit under test and therefore the fault tolerance threshold is  $t = \left\lfloor \frac{d-1}{2} \right\rfloor$ , and  $t+1$  is the onset weight. This makes sense for our SID error model: since no correlated Pauli errors are introduced, the mapping from injected faults to Pauli weight is faithful, and Equation 4 is accurate when stated in terms of Pauli weight. Thus, we are free from the concern of determining the onset weight.

*The onset weight  $t+1$  is known.*

In our experiments, IBM's S-curve model fits the observed data well, but its extrapolation to low-weight subspaces near the fault-tolerant threshold exhibits low precision in our noise model. Moreover, the contribution to the logical error rate is dominated by these low-weight subspaces, so it directly results in low accuracy in the logical error rate estimation, as we show experimentally in Section 8.3. This motivated us to design a more accurate model.

The key idea in our S-curve model is to introduce a special point at  $w = t$  in the denominator of the S-curve model, encoding that, in our SID noise model, the logical error rate is exactly zero for all subspaces with  $w \leq t$ . We also carefully model the extrapolation towards the singular point  $w = t$  to achieve good agreement with the data.

**Definition 3** (Our S-Curve Model). *For a given integer  $t \geq 0$ , intended to be  $t = \frac{d-1}{2}$ , the function*

Code [[n,k,d]]	Our Model $R^2$	IBM Model $R^2$
Surface [[9,1,3]]	0.9902	0.9919
Surface [[25,1,5]]	0.9984	0.9982
Surface [[49,1,7]]	0.9989	0.9986
Toric [[18,2,3]]	0.9900	0.9909
Toric [[50,2,5]]	0.9965	0.9966
Toric [[98,2,7]]	0.9977	0.9978
BB code [[72,12,6]]	0.9939	0.9935
BB code [[90,8,10]]	0.9956	0.9960
BB code [[108,8,8]]	0.9962	0.9963

Table 2:  $R^2$  comparison between our model and the IBM model across codes calculated from data in Figure 4. This result indicates that both S-curve models are well justified to be used to learn and evaluate the quantum error correction circuits.

$f_t^{ours}$  is described by three real parameters  $\mu, \alpha, \beta$ , and takes as input an integer  $w \geq 0$ :

$$f_t^{ours}[\mu, \alpha, \beta](w) = \begin{cases} \frac{1}{2} \cdot \frac{1}{1 + e^{-\frac{w-\mu}{\alpha} + \frac{\beta}{\sqrt{(w-t)}}}} & t < w \\ 0 & w \leq t \end{cases}$$

Our model approximates each  $P_L^w$  by  $f_t^{ours}[\mu, \alpha, \beta](w)$ . Notice that we model the fault-tolerant zone by defining  $f_t^{ours}[\mu, \alpha, \beta](w) = 0$  for  $w \leq t$ . One can easily check that  $f_t^{ours}[\mu, \alpha, \beta]$  satisfies the requirements in Definition 1.

### Fitting an S-Curve to QEC-Test Data.

Given the QEC-test data in Figure 2, we use the least-squares method to fit an S-curve to the data and determine the parameters. We do this for both IBM's and our S-curve models, resulting in the curves shown in Figure 4 and the  $R^2$  values shown in Table 2, which are all close to 1. For example, for the surface code with distance 7 (discussed in Sections 1–2), the curve-fitting produces these parameters for our S-curve model:  $\mu = 41.71$  and  $\alpha = 19.93$  and  $\beta = 16.03$ . The resulting  $f_t[\mu, \alpha, \beta]$  function fits the data in Figure 4 almost perfectly:  $R^2 = 0.9989$ . The consistent high quality of the fits across distinct code families supports the generality, robustness, and prediction power of the two S-curve models. We can use this to our advantage, as we consider next.

## 4 Separating Low and High Weights

In this section, we define the boundary between the low weights and the high weights, and define an upper bound on the high weights. We call those weights  $w_{\text{sweet}}$  (the sweet spot) and  $w_{\text{sat}}$  (the saturation point):

$$1 \leq \text{low weights} < w_{\text{sweet}} \leq \text{high weights} \leq w_{\text{sat}}$$

For a function  $f$  that satisfies the requirements of Definition 1, we define  $w_{\text{sweet}}$  and  $w_{\text{sat}}$  as follows:

$$y(w) = \ln\left(\frac{1}{2f(w)} - 1\right) \quad (6)$$

$$w_{\text{sweet}} = \max\{w \in \mathbb{N} \mid y''(w) \geq \Gamma|y'(w)|\} \quad (7)$$

$$w_{\text{sat}} = \max\{w \in \mathbb{N} \mid f(w) < 0.25\} \quad (8)$$

We introduce  $\Gamma$  as the knob to control accuracy versus cost.  $\Gamma$  is a hyperparameter with a default value  $\Gamma = 1$ . The idea behind the definition of  $w_{\text{sweet}}$  lies in the transformed curve  $y(w)$  that we define in Equation 6 and illustrate in Figure 5 for our running example of a surface code with distance 7. We call this curve a Y-curve.

If we plug our S-curve model in Definition 3 into Equation 6, we get, for  $t < w$ :

$$\begin{aligned} y_t[\mu, \alpha, \beta](w) &= \ln\left(\frac{1}{2f_t[\mu, \alpha, \beta](w)} - 1\right) \\ &= -\frac{1}{\alpha}w + \frac{\mu}{\alpha} + \frac{\beta}{\sqrt{w-t}} \end{aligned}$$

The function  $y_t$  has linear and non-linear components. We provide a physical interpretation for this behavior. The linear term  $-\frac{1}{\alpha}w + \frac{\mu}{\alpha}$ , captures the overall degradation of error-correcting performance as the error weight  $w$  increases. The non-linear term,  $\frac{\beta}{\sqrt{w-t}}$ , models the increased ability of the QEC circuit to correct low-weight errors.

The first-order derivative of  $y_t$  is

$$y'_t(w) = -\frac{1}{\alpha} - \frac{\beta}{2} \frac{1}{(w-t)^{\frac{3}{2}}}, \quad \lim_{w \rightarrow \infty} y_t(w) = -\frac{1}{\alpha}$$

In the formula above for  $y'_t(w)$ , the first term says that the almost-linear portion of the curve has slope  $-\frac{1}{\alpha}$ . The second term is non-linear but diminishes quickly as  $w$  increases. The second-order derivative of  $y_t$  is:

$$y''_t(w) = \frac{3\beta}{4} \frac{1}{(w-t)^{\frac{5}{2}}}, \quad \lim_{w \rightarrow \infty} y''_t(w) = 0 \quad (9)$$

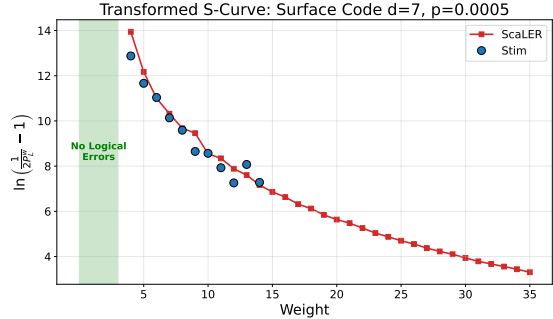


Figure 5: Y-curve transformation of (c) via  $\ln\left(\frac{1}{2P_L^w} - 1\right)$  (Eq. 6); blue: Stim; red: ScaLER.

We are looking for a sweet spot where the second order derivative is comparable with the absolute value of the first order derivative, that is, well before the second-order derivative gets close to 0. This leads us to Equation 7, which defines  $w_{\text{sweet}}$  so that we have

$$y''(w_{\text{sweet}}) \approx \Gamma|y'(w_{\text{sweet}})|$$

The idea behind the definition of  $w_{\text{sat}}$  is to ensure that we will focus on the weights that are in the left half of the S-curve. Ideally, we would define  $w_{\text{sat}}$  as the inflection point where the steep slope ends and the S-curve starts to flatten out. Mathematically, this means that we want  $w_{\text{sat}}$  to satisfy  $f''(w_{\text{sat}}) \approx 0$ . Instead, Equation 8 is a more practical and approximate definition of the inflection point. From Definition 1, we know that  $f(w)$  increases from 0 to 0.5, and from Figure 4 we see that the inflection point is roughly when  $f(w)$  is half way between 0 and 0.5, which is 0.25. So, we define  $w_{\text{sat}}$  so that it satisfies

$$f(w_{\text{sat}}) \approx 0.25$$

For example, for the surface code with distance 7 (discussed in Sections 1–3), if we use our S-curve model in Definition 3, fitted to the QEC-test data as described in Section 3, we get  $w_{\text{sweet}} = 12$  and  $w_{\text{sat}} = 65$ . We will test only high-weight samples, which for this example are the ones with weights between 12 and 65.

## 5 Testing Samples with High Weights

Our approach focuses on testing samples with high weights and then extrapolating to low weights. The idea is to test samples with weights between  $w_{\text{sweet}}$  and  $w_{\text{sat}}$ , and obtain values for

Algorithm 1: ADAPSAM — Stratified and adaptive subspace sampling algorithm for S-curve fitting

---

**Require:** Total sampling budget  $S_{\max}$ , Y-curve model template  $y_t[\vec{v}]$ , minimum logical errors per subspace  $N_{LE}$ , hyperparameter  $\Gamma$ .

**Ensure:** Fitted parameter  $\vec{v}$  of Y-curve model.

- 1: **procedure** ADAPSAM( $S_{\max}, N_{LE}, \Gamma$ )
- 2:   **Stage 1: Binary-search stage**
- 3:    $w_{\text{err}} \leftarrow$  smallest  $w$  with observed logical errors with 1,000 samples (binary search)
- 4:    $w_{\text{sat}} \leftarrow$  largest  $w$  with  $\hat{P}_L(w) \leq 0.25$  (binary search)
- 5:   **Stage 2: Initial-sampling stage**
- 6:    $\mathcal{W} \leftarrow 5$  points in  $[w_{\text{err}}, w_{\text{sat}}]$ , uniformly
- 7:   **for all**  $w \in \mathcal{W}$  **do**
- 8:     Sample at  $w$  until  $N_{LE}$  logical errors are collected
- 9:   **end for**
- 10:    $w_{\text{front}} \leftarrow \min(\mathcal{W})$
- 11:   **Stage 3: Iterative stage.**
- 12:   **while**  $|\mathcal{W}| < 10 \wedge \#\text{samples} \leq S_{\max}$  **do**
- 13:     Fit Y-curve:  $\vec{v} \leftarrow \text{FIT YCURVE}(\text{data})$
- 14:      $\hat{w}_{\text{sweet}} \leftarrow \max\{w \mid y''(w) \geq \Gamma|y'(w)|\}$
- 15:     **if**  $w_{\text{front}} \leq \hat{w}_{\text{sweet}}$  **then break**
- 16:     **end if**
- 17:      $\Delta w \leftarrow \lfloor (w_{\text{err}} - \hat{w}_{\text{sweet}})/5 \rfloor$
- 18:      $w_{\text{new}} \leftarrow \max(w_{\text{front}} - \Delta w, \hat{w}_{\text{sweet}})$
- 19:     Sample at  $w_{\text{new}}$  until  $N_{LE}$  logical errors collected
- 20:      $\mathcal{W} \leftarrow \mathcal{W} \cup \{w_{\text{new}}\}; w_{\text{front}} \leftarrow w_{\text{new}}$
- 21:   **end while**
- 22:   Fit final Y-curve.
- 23:   **return** Fitted parameters  $\vec{v}$ .
- 24: **end procedure**

---

the model parameters in the S-curve model. The challenge is that this is circular: we want to use  $w_{\text{sweet}}$  and  $w_{\text{sat}}$  to determine  $f$ , but we need  $f$  to determine  $w_{\text{sweet}}$  and  $w_{\text{sat}}$ . In this section, we explain how we break this cycle and successfully test within a limited time budget.

## 5.1 Our Approach

Our approach is described in Algorithm 1 and illustrated in Figure 6. The idea is to test samples with lower and lower weights, proceeding in three stages.

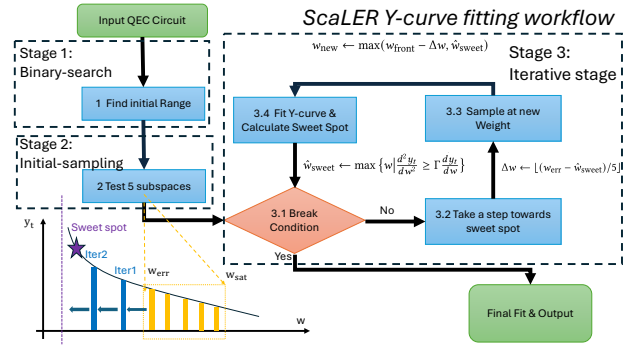


Figure 6: Diagram for the adaptive Y-curve fitting approach used in ScaLER.

For a weight  $w$ , we will refer to the set of samples with weight  $w$  as a subspace.

**The binary-search stage.** In the first stage, we use binary search to determine both  $w_{\text{sat}}$  and also a weight  $w_{\text{err}}$  that satisfies the following:

$$P_L^{w_{\text{err}}} \approx 0.001$$

For QEC-implementations with high distances, we have  $w_{\text{sweet}} < w_{\text{err}} < w_{\text{sat}}$ . We use 1,000 samples for each weight, so  $w_{\text{err}}$  is a weight for which testing 1,000 samples gives a single logical error, while  $w_{\text{sat}}$  is a weight for which testing 1,000 samples gives less than 250 errors.

**The initial-sampling stage.** In the second stage, we test in 5 subspaces that are evenly distributed between  $w_{\text{err}}$  and  $w_{\text{sat}}$ , and we fit a Y-curve to the data. From the Y-curve we estimate  $w_{\text{sweet}}$ .

**The iterative stage.** In the third stage, we test in 5 subspaces that are evenly distributed between  $w_{\text{sweet}}$  and  $w_{\text{err}}$ . Each time we finish a subspace, we update the Y-curve and update the estimate of  $w_{\text{sweet}}$ . Testing concludes either when 5 subspaces have been tested or when the time budget is exhausted.

**Stopping criterion per subspace.** We generate random samples in a given subspace until more than  $N_{LE}$  logical errors are observed. The default is  $N_{LE} = 30$ .

## 5.2 Example

For the surface code with distance 7 (discussed in Sections 1–4), Algorithm 1 proceeds as follows.

Symbol	Description
$S_{\max}$	Total sampling budget (equivalent to a time budget)
$N_{LE}$	Required logical errors per subspace (set to 30 in this paper)
$\Gamma$	Sweet-spot curvature threshold (Eq. 4) (set to 1 in this paper)

Table 3: Hyperparameters in ADAPTIVESAMPLING.

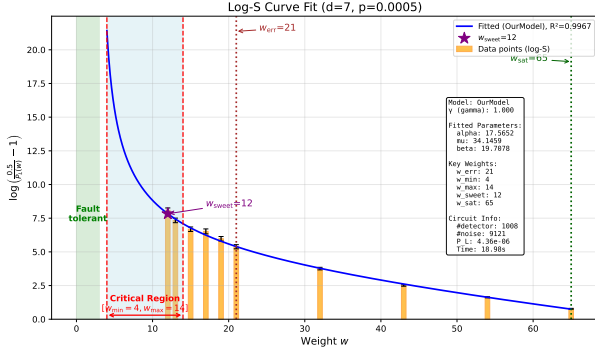


Figure 7: Examples of fitted curves for the surface code with distance 7 when  $p = 0.0005$ .

**Compilation.** A distance- $d$  surface code uses  $2d^2 - 1$  qubits. Therefore, our distance-7 surface code involves a 97-qubit circuit that contains 1008 detectors. We repeat each stabilizer-measurement round  $3d = 21$  times to preserve fault tolerance in the circuit-level noise model [27].

In the SID noise model, we consider all fault locations in the circuit. This circuit has  $n = 9,121$  locations, and we compile the corresponding quantum error propagation graph (QEPPG), stored as a  $9,121 \times 1008$  matrix that represents the propagation of Pauli errors to the detectors.

**The binary-search stage.** The range of binary search is  $1 \leq w \leq 9,121$ . For each subspace with weight  $w$  that we encounter in the search, we generate 1,000 random samples. The outcome is that we find  $w_{\text{err}} = 21$  and  $w_{\text{sat}} = 65$ .

**The initial-sampling stage.** We test in the five subspaces with weights

$$w_{\text{err}} = 21 \leq 32 \leq 43 \leq 54 \leq 65 = w_{\text{sat}}$$

Table 4 shows the results. For example, for the subspace with weight 21, we test 18,333 samples and observe 42 logical errors. The outcome is that we estimate  $w_{\text{sweet}} = 13$ .

Weight	$N_w^{\text{LE}}$	$N_w^{\text{Test}}$	$\hat{P}_L^w$
$w_{\text{sweet}} = 12$	32	207,499	$1.54 \times 10^{-4}$
	35	107,499	$3.26 \times 10^{-4}$
	36	57,499	$6.26 \times 10^{-4}$
	30	40,833	$7.35 \times 10^{-4}$
	36	28,333	$1.27 \times 10^{-3}$
$w_{\text{err}} = 21$	42	18,333	$2.29 \times 10^{-3}$
	114	10,000	$1.14 \times 10^{-2}$
	377	10,000	$3.77 \times 10^{-2}$
	821	10,000	$8.21 \times 10^{-2}$
$w_{\text{sat}} = 65$	1579	10,000	$1.58 \times 10^{-1}$

Table 4: Logical error statistics per error weight  $w$ . Here  $N_w^{\text{LE}}$  is the number of observed logical errors,  $N_w^{\text{Test}}$  is the total number of trials, and  $\hat{P}_L^w = N_w^{\text{LE}} / N_w^{\text{Test}}$  is the estimated logical error rate.

**The iterative stage.** We tested a succession of subspaces and kept updating our estimate of  $w_{\text{sweet}}$ . Eventually, we estimated  $w_{\text{sweet}} = 12$ , after testing the five subspaces with weights

$$w_{\text{sweet}} = 12 \leq 13 \leq 15 \leq 17 \leq 19 < w_{\text{err}}$$

Table 4 shows the results.

We fit a Y-curve to the data. For our S-curve model, we estimate the parameters as  $\hat{\alpha} = 17.57$ ,  $\hat{\mu} = 34.14$ , and  $\hat{\beta} = 19.71$ .

**Comparison with Stim.** Figure 2 presents Stim data from testing the distance-7 surface code, where we instrumented Stim with additional logging hooks and ran the simulator for a two-hour time budget and observed 503 logical errors.

Stim uses 83,000,000 samples to observe 503 logical errors. In contrast, ScaLER uses approximately  $5 \times 10^5$  samples in total, that is, only 0.6% of Stim’s sample count. Table 4 shows that most of the sampling budget of ScaLER is concentrated on the two smallest weights near the sweet spot, namely 12 and 13. For these weights, the subspace logical error rate is low and therefore hard to estimate. However, Figure 2 shows that Stim primarily tests subspaces with weights between 1 and 10, which are significantly more difficult to test than subspaces with the higher weights 12 and 13.

---

Algorithm 2: SCALER — Stratified fault injection and S-Curve Fitting for Logical-Error-Rate Estimation

---

**Require:** Circuit  $\mathcal{C}$  with circuit-level code distance  $d$ , physical error rate  $p$ , total sample budget  $S_{\max}$ , and total error budget  $N_w^{LE}$ , sweet-spot curvature threshold  $\Gamma$ .

**Ensure:**  $\hat{P}_L$

- 1: **procedure** SCALER( $\mathcal{C}, d, p, S_{\max}, N_w^{LE}, \Gamma$ )
- 2:    $t \leftarrow \frac{d-1}{2}$
- 3:    $\vec{v} \leftarrow \text{ADAPSAM}(S_{\max}, N_w^{LE}, \Gamma)$
- 4:    $n \leftarrow \text{number of locations in } \mathcal{C}$
- 5:    $\sigma \leftarrow \sqrt{np(1-p)}$
- 6:    $w_{\min} \leftarrow \lfloor np - 5\sigma \rfloor; w_{\max} \leftarrow \lceil np + 5\sigma \rceil$
- 7:    $\hat{P}_L = \sum_{w=w_{\min}}^{w_{\max}} f_t[\vec{v}](w) \cdot \binom{n}{w} p^w (1-p)^{n-w}$
- 8:   **return**  $\hat{P}_L$
- 9: **end procedure**

---

## 6 Our Algorithm

In this section, we present our overall algorithm ScaLER (which abbreviates Scalable Logical Error Rate testing). The idea is to first test samples with high weights and derive an S-curve that models the test data, and then use the S-curve to estimate the logical error rate.

### 6.1 Pseudo-code for Our Algorithm

Algorithm 2 presents pseudo-code for our algorithm. The input consists of a QEC circuit  $\mathcal{C}$  with a circuit-level code distance  $d$ , the physical error rate  $p$ , the total sample budget  $S_{\max}$ , the maximum number of logical errors  $N_w^{LE}$  to sample in one subspace  $N$ , and the sweet-spot curvature threshold  $\Gamma$ .

In line 2, we calculate the maximum number of errors that  $\mathcal{C}$  is designed to correct.

In line 3, we run our testing procedure from Section 5, which produces the S-curve parameters.

In line 4, we calculate the number of locations in the circuit  $\mathcal{C}$ .

In line 5, we calculate the standard deviation of the probability distribution that models quantum-hardware errors. For a large circuit, the number of errors follows a binomial distribution with standard deviation  $\sigma \approx \sqrt{np(1-p)}$ .

In line 6, we calculate the weight interval that we will use to estimate the logical error rate. We

know that 99.99994% of the mass of the distribution lies within  $[np - 5\sigma, np + 5\sigma]$ . We will use the term *critical region* to refer to the interval  $[np - 5\sigma, np + 5\sigma]$ .

In line 7, we estimate the logical error rate by applying Equation 3, with  $P_L^w$  replaced by the model  $f_t[\vec{v}]$ .

Finally, in line 8, we return the estimated  $\hat{P}_L$ .

### 6.2 Example

For our running example of a surface code with distance 7 (discussed in Sections 1–5), we have a circuit with  $n = 9,121$  locations and we have the physical error rate  $p = 0.0005$ . The expected number of injected errors is  $\mu = np = 9,121 \cdot 5 \cdot 10^{-4} \approx 4$ , with the standard deviation  $\sigma = \sqrt{np(1-p)} \approx \sqrt{9,121 \cdot 5 \times 10^{-4}(1 - 5 \cdot 10^{-4})} \approx 2$ . Using a coverage factor  $k = 5$ , we define the critical error-weight region as  $[\mu - k\sigma, \mu + k\sigma] \approx [4 - 5 \cdot 2, 4 + 5 \cdot 2]$ . Since the error weight below 3 is in the fault-tolerant zone, we set the lower bound to 4. The critical region (blue color in Figure 7) is therefore  $[w_{\min} = 4, w_{\max} = 14]$ . Lines 2–3 of Algorithm 2 produce the S-curve  $f_t[17.57, 34.14, 19.71](w)$ , after which lines 4–7 produce the following estimate of the logical error rate:

$$\begin{aligned} \hat{P}_L &= \sum_{w=4}^{24} f_t[17.57, 34.14, 19.71](w) \binom{9,121}{w} \\ &\quad \cdot (5 \times 10^{-4})^w (1 - 5 \times 10^{-5})^{n-w} \\ &\approx 4.36 \times 10^{-6}. \end{aligned} \quad (10)$$

The estimated logical error rate for Stim is  $\frac{503}{83,000,000} \approx 6.06 \times 10^{-6}$ . ScaLER is off by 28%, compared to Stim in this case. We will further explain the cause of the inaccuracy and how to improve in Section §8.2.

## 7 Implementation

We implemented ScaLER in C++ and Python. The C++ part encodes the error model and compiles each sample in a manner similar to Stim [13]. In particular, it compiles a circuit to a binary graph that we call a quantum error propagation graph (QEPPG) in which every vertex is a Pauli gate and each edge denotes a type of propagation, as illustrated in Figure 8. In addition, it uses binary vector addition to simulate Pauli

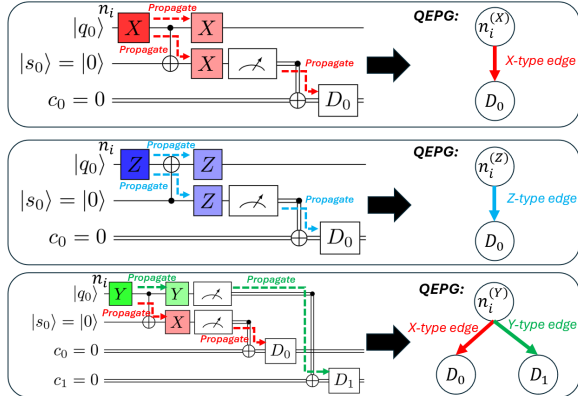


Figure 8: Construction of a QEPG graph in ScaLER.

error propagation, uses Boost’s dynamic\_bitset [36] to represent and update the QEPG graph, and accelerates the computation by parallelizing across threads with OpenMP [37].

The Python part implements Algorithms 1–2, exposing the generated samples to Python as NumPy arrays using pybind11 [38] and using the Python scipy library [39] to fit the Y-curve model and calculate the logical error rate.

**Access.** We have released ScaLER as an open-source project on GitHub, including a README file that explains how to install our tool, run it, and reproduce all the results in this paper.

## 8 Evaluation

Our experimental evaluation answers three research questions (RQs) about our approach. The questions and our answers are as follows.

- RQ1 **Does ScaLER scale better than Stim?** Yes, at the physical error rate 0.0005 with a time budget of 2 hours, Stim cannot sample any logical error with a two hour time budget for distance 13. ScaLER scaled to distance 17.
- RQ2 **Does ScaLER agree with Stim?** Yes, more than half of the results have an inaccuracy below 20%. For the remaining cases, we show that the accuracy can be improved by changing the hyperparameter settings.
- RQ3 **What is the best S-curve model?** We tested both IBM’s S-curve model and variants of our S-curve model and found that our model with  $\Gamma = 1$  achieves the highest accuracy.

In the remainder of this section, we show how our evaluation results support our claims.

**Benchmarks.** We experiment with both standard topological codes and QLDPC codes. Our benchmarks are three sets of QEC programs from previous work: the standard surface code and the Toric code with distances up to 17, from the Gidney artifact [13], and four different Bivariate Bicycle QLDPC codes [40] with distances up to 12, from Perlin et al. [41].

The Surface code, Toric code, and variants are decoded by Pymatching [42], the Bivariate Bicycle Qldpc code is decoded by the Belief Propagation with Ordered Statistics Decoding (BP-OSD) algorithm [43].

We set the physical error rate at  $p = 0.0005$  for most experiments, except where noted explicitly. This rate is a realistic setting because many platforms have a physical error rate for 1-qubit gates that is below  $10^{-3}$  [44, 45, 46, 47, 48, 49].

**Experimental Setup.** We conducted all experiments on a Windows desktop with an Alienware Aurora R16 platform, equipped with a 13th Gen Intel Core i9-13900F processor (24 cores, 32 threads) and 32 GB of RAM. We set a time budget of 2 hours for each experiment. We repeated each experiment 5 times, which allowed us to compute the average value and the standard deviation. For each experiment, we record the number of samples, the execution time, and the logical error rate.

**Stopping criterion for Stim** Following previous work, we run Stim until it observes 100 logical errors or exhausts the 2-hour time budget [23]. The threshold of 100 logical errors ensures that the resulting statistical uncertainty, measured by relative standard deviation (standard deviation divided by mean estimated value) is less than 10% [50]. ScaLER matches this.

We compute the relative accuracy of the logical error rate estimated by ScaLER versus Stim for all configurations in which Stim observes at least 100 logical errors, and thus its estimated logical error rate has high statistical confidence and can be considered as ground truth.

### 8.1 RQ1: Scalability Comparison

Table 5 shows the results for all our benchmarks.

$p = 0.0005$							
Code	d	Stim LER	Stim Sampled LE	Stim (s)	ScaLER LER	ScaLER (s)	Rel. error
BBCode[[72, 12, 6]]	6	$(3.76 \pm 0.12) \times 10^{-4}$	102	562	$(4.40 \pm 0.45) \times 10^{-4}$	559	-17.0%
BBCode[[90, 8, 10]]	10	$(8.68 \pm 0.36) \times 10^{-5}$	100	6839	$(1.01 \pm 0.04) \times 10^{-4}$	5447	-16.4%
BBCode[[108, 8, 8]]	8	$(5.89 \pm 1.29) \times 10^{-6}$	8	7200	$(4.20 \pm 0.70) \times 10^{-6}$	6044	(28.7%)
BBCode[[144, 12, 12]]	12	0	0	7200	$(4.16 \pm 0.86) \times 10^{-6}$	7065	—
$p = 0.0001$							
Code	d	Stim LER	Stim Sampled LE	Stim (s)	ScaLER LER	ScaLER (s)	Rel. error
BBCode[[72, 12, 6]]	6	$(2.47 \pm 0.3) \times 10^{-6}$	19	7200	$(1.02 \pm 0.65) \times 10^{-6}$	2436	(-58.7%)
BBCode[[90, 8, 10]]	10	$(6.59 \pm 2.7) \times 10^{-7}$	2	7200	$(2.58 \pm 1.0) \times 10^{-7}$	6686	(-60.8%)
BBCode[[108, 8, 8]]	8	0	0	7200	$(5.43 \pm 0.83) \times 10^{-11}$	6795	—
BBCode[[144, 12, 12]]	12	0	0	7200	$(4.93 \pm 0.13) \times 10^{-12}$	6209	—

Code	d	Stim LER	Stim Sampled LE	Stim (s)	ScaLER LER	ScaLER (s)	Rel. error
Surface	3	$(5.77 \pm 0.19) \times 10^{-4}$	184	0.34	$(5.81 \pm 0.60) \times 10^{-4}$	0.83	-0.7%
	5	$(6.41 \pm 0.35) \times 10^{-5}$	115	8.7	$(3.98 \pm 0.38) \times 10^{-5}$	4.6	37.9%
	7	$(5.95 \pm 0.66) \times 10^{-6}$	101	216	$(3.70 \pm 0.27) \times 10^{-6}$	20	37.8%
	9	$(3.59 \pm 0.59) \times 10^{-7}$	36	3116	$(3.52 \pm 0.44) \times 10^{-7}$	95	2.0%
	11	$(2.22 \pm 1.26) \times 10^{-8}$	3	7213	$(2.92 \pm 0.25) \times 10^{-8}$	3337	(31.5%)
	13	0	0	7200	$(2.44 \pm 0.17) \times 10^{-9}$	6287	—
	15	0	0	7200	$(1.64 \pm 0.23) \times 10^{-10}$	7200	—
	17	0	0	7200	$(1.51 \pm 0.07) \times 10^{-11}$	7200	—
Toric	3	$(7.05 \pm 0.35) \times 10^{-4}$	159	0.16	$(7.51 \pm 0.21) \times 10^{-4}$	0.85	-6.5%
	5	$(8.32 \pm 0.47) \times 10^{-5}$	125	5.9	$(4.40 \pm 0.25) \times 10^{-5}$	4.7	47.1%
	7	$(6.82 \pm 0.54) \times 10^{-6}$	101	162	$(4.43 \pm 0.20) \times 10^{-6}$	20	35.0%
	9	$(4.56 \pm 0.38) \times 10^{-7}$	100	1998	$(4.23 \pm 0.29) \times 10^{-7}$	125	7.2%
	11	$(3.53 \pm 1.6) \times 10^{-8}$	5	7200	$(3.62 \pm 0.15) \times 10^{-8}$	2282	(2.55%)
	13	0	0	7200	$(2.46 \pm 0.22) \times 10^{-9}$	5483	—
	15	0	0	7200	$(2.27 \pm 0.19) \times 10^{-10}$	7200	—

Table 5: Comparison of LER estimation: Stim vs. ScaLER. (Top) BB codes at  $p = 0.0005$  and  $p = 0.0001$ . (Bottom) Surface and Toric codes at  $p = 0.0005$ . We use a 2-hour time budget; BB is repeated 3 times and Surface/Toric is repeated 5 times. For larger instances, Stim observes no logical errors within budget, while ScaLER still produces an estimate.

**Result for Surface code and Toric code.** We evaluated the logical error rates for both the Surface and Toric codes with code distances up to  $d = 17$ . For distance  $d \leq 10$ , Stim successfully sampled sufficient logical errors within time budget, producing estimates with small standard deviations and high statistical confidence. However, as the code distance increases, Stim struggles to observe rare error events.

In contrast, ScaLER consistently produces high-confidence logical error rate estimates up to  $d = 17$  with a 2-hour time budget.

For example, at the code distance  $d = 11$  for the Surface code, Stim observed only 3 logical errors after 2 hours, resulting in a standard deviation exceeding 50% of the estimated value. In contrast, ScaLER provided an estimate of  $(2.92 \pm 0.25) \times 10^{-8}$  with high confidence in less than 1 hour.

The results demonstrate that ScaLER is signifi-

cantly more scalable than Stim. While Stim effectively reached its computational limit at  $d = 10$ , ScaLER remains robust at higher distances. In particular, ScaLER successfully characterized the Surface code at  $d = 17$ , measuring a logical error rate of  $1.51 \times 10^{-11}$ , in 2 hours on a desktop. This logical error rate approaches the scale required for real-world quantum applications, such as factoring 2,048-bit RSA integers [51].

**Result for Bivariate Bicycle code.** We present the results for the Bivariate Bicycle codes in the top of Table 5. We emphasize that the BP-OSD LDPC decoder is significantly slower than the standard Pymatching decoder, making simulation computationally demanding even at small scales.

The rows in Table 5 are ordered by code size. For the first two entries, BBCode [[72,12,6]] and BBCode [[90,8,10]], Stim produces logical error

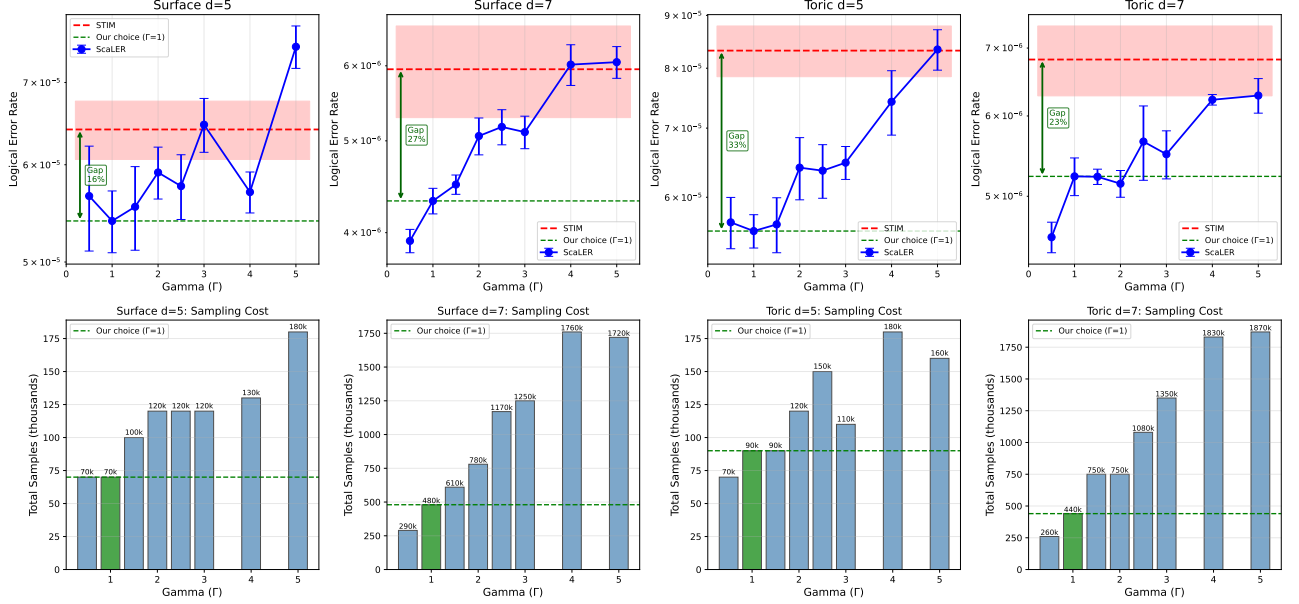


Figure 9: We measure the accuracy-cost tradeoff of different Hyperparameter  $\Gamma$  selection of our algorithm at small scale when code distance is 5 and 7. Above: We plot the logical error rate estimated by ScaLER at different  $\Gamma$  together with output of STIM. Below: We plot the total sampling cost of different Hyperparameters. When  $\Gamma$  increases, ScaLER gets logical error rate closer to STIM, with a large sampling cost. At  $\Gamma = 1$ , we save a tremendous amount of sampling cost while has an inaccuracy around 20%, which is acceptable.

rate estimates (on the order of  $10^{-4}$ ) with low standard deviations, successfully sampling over 100 logical errors.

For the larger BBCode  $[[108,8,8]]$ , Stim is unable to sample the 100 logical errors that were targeted within the 2-hour time budget. In fact, only 8 logical errors were observed, resulting in a dramatic increase in the standard deviation of the estimate.

For the largest code, BBCode  $[[144,12,12]]$ , Stim fails to observe any logical errors and cannot produce a meaningful estimate. In contrast, ScaLER scales effectively, maintaining valid and robust estimates for both cases.

**Lower Physical Error Rate.** To further stress-test the scalability of the tools in the low-error regime, we also did experiments with the lower physical error rate of  $p = 0.0001$ . The result in Table 5 indicates that Stim faces significant challenges in this lower error rate regime. Within the time budget of two hours, Stim observes only 19 logical errors for BBCode  $[[72,12,6]]$ , and just 2 for BBCode  $[[90,8,10]]$ , while failing to observe any logical errors for the remaining larger code instances.

In contrast, ScaLER successfully produces logical error rate estimates for all four codes. The results demonstrate that ScaLER exhibits superior scalability compared to Stim, particularly as the physical error rate is further reduced.

## 8.2 RQ2: Agreement Check

To evaluate the accuracy of ScaLER, we compute the relative accuracy of its estimated logical error rates with respect to the baseline results from Stim.

**Relative error compared with Stim.** As shown in Table 5, ScaLER demonstrates strong agreement with Stim under our default hyperparameter setting  $\Gamma = 1$ . Indeed, the logical error rate is consistent with Stim in order of magnitude with acceptable accuracy. For BBCode  $[[72,12,6]]$  and BBCode  $[[90,8,10]]$  at  $p = 0.0005$ , where Stim observes 100 logical errors within time budget, the inaccuracy of ScaLER compared with Stim is below 20%.

For the surface code and the toric code with distance 3 and 9, the inaccuracy is below 10%.

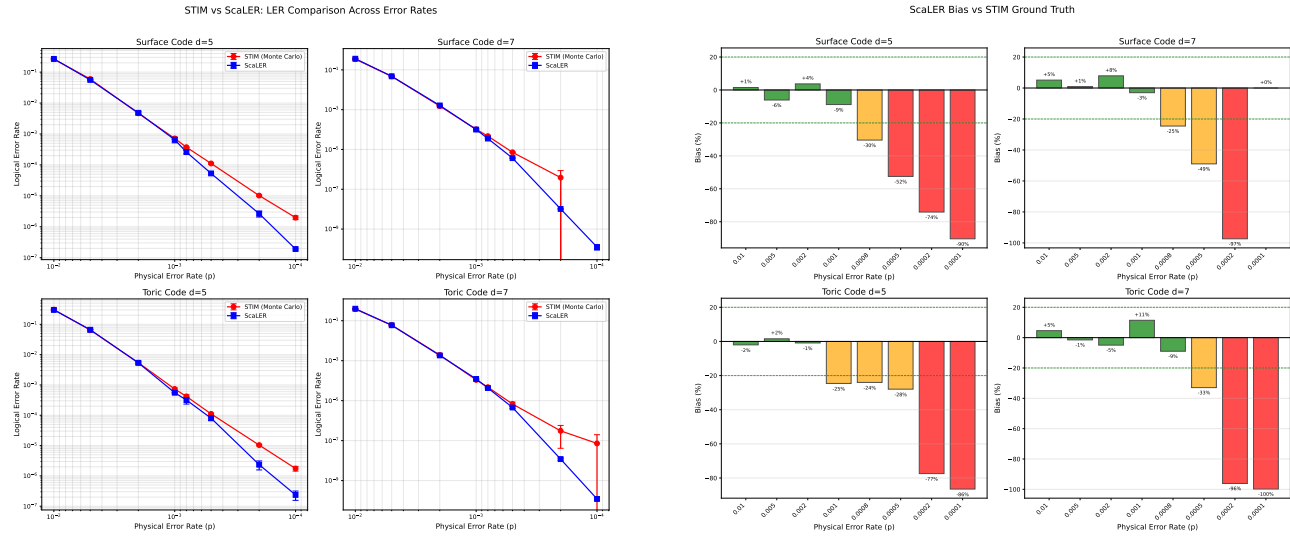


Figure 10: Study of the relative error of ScaLER compared with Stim under different physical error rate ranges from  $p = 0.01$  to  $0.0001$  on Surface code and Toric code. Left figure shows the plot of logical error rate plot of both method, and the right figure shows the relative accuracy of ScaLER compared with Stim. First, we observe that both results match well for higher physical error rate, but the accuracy starts to decrease when for lower physical error rate. Second, the results also suggest that the current hyper parameter setting is acceptable if the goal is to achieve a inaccuracy below 20%.

**Accuracy-cost tradeoff due to sweet spot selection.** We observe a larger inaccuracy of approximately 40% for the Toric and Surface codes at distances  $d = 5$  and  $d = 7$ . Although this margin of error is generally acceptable for establishing the order of magnitude, it may be insufficient for applications requiring high-precision estimates. In this section, we investigate the source of this discrepancy and propose a systematic method to reduce it within our framework.

In Section 4, we define the sweet spot as:

$$y''(w_{\text{sweet}}) \approx \Gamma |y'(w_{\text{sweet}})|$$

In our previous evaluation, we used the default setting  $\Gamma = 1$  for all experiments. If we increase  $\Gamma$ , we shift the sweet spot toward lower weights. Although this requires a significantly higher testing effort, it allows us to extract more information from low-weight subspaces, resulting in logical error rate estimates with higher accuracy.

As shown in Figure 9, increasing  $\Gamma$  consistently increases the accuracy at the expense of higher sampling costs, validating our hypothesis. We therefore conclude that the low accuracy observed earlier stems from a suboptimal selection of the sweet spot for these two cases. If a more accurate estimate is required and sufficient computational budget is available, one can increase  $\Gamma$ .

**Relative error at different physical error rates.** To validate the robustness of our method under different physical error rates, we extend our evaluation over a physical error rate range of  $p = 0.0001$  to  $p = 0.01$ .

We evaluated both the surface code and the toric codes at distance  $d = 5$  and  $d = 7$  using both tools. As illustrated in Figure 10, we observe an increase in the discrepancy between ScaLER and Stim as the physical error rate decreases.

This phenomenon can be explained by the three scenarios shown in Figure 11. Specifically, for moderate error rate ( $p = 0.001$  and  $p = 0.002$ ), our sweet spot selection accurately fits the curve and extrapolates to the critical subspaces which contribute to the logical error rate. However, when the physical error is much smaller (such as  $p = 0.0002$ ), most errors are concentrated at low weights, where the curve extrapolation is less reliable.

**Summary.** Our results show that ScaLER produces estimates that are highly consistent with those of Stim. Furthermore, the observed inaccuracy can be explained through a geometric interpretation and can be systematically reduced, given a larger computational budget.

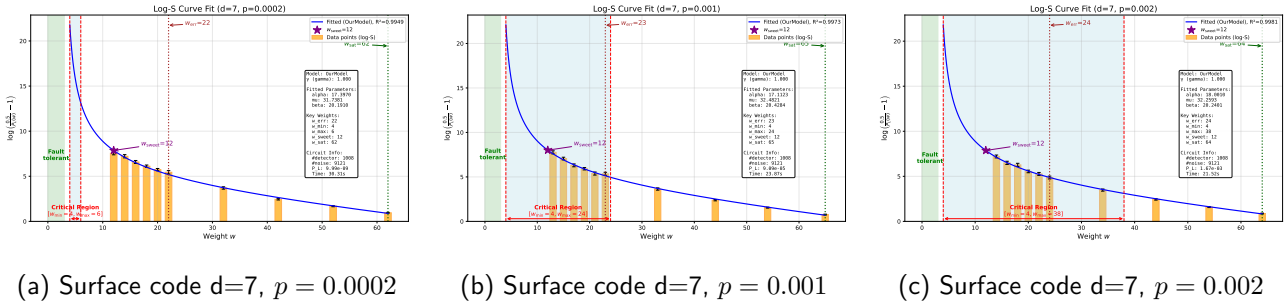


Figure 11: The result of testing the same Surface code circuit with distance 7 under three different physical error rate 0.0002, 0.001, 0.002. The blue region highlight the critical weights $[np - 5\sigma, np + 5\sigma]$  that distribute to logical error rate. Although ScaLER tests enough subspaces towards the sweet spot in all three cases, the accuracy for  $p = 0.0002$  is much lower than for the other two because our definition of sweet spot is far from the actual critical weights.

### 8.3 RQ3: S-curve Comparison

We compare the effectiveness of IBM’s S-curve model, our S-curve model, and three variants of our S-curve model to justify the model design in this research. First, we run our algorithm with IBM’s model.

**Effectiveness of IBM’s model.** The logical error rates predicted by IBM’s model are reported in Table 7. Across all configurations, IBM’s model is less accurate than our S-curve model. Figure 13 compares the corresponding Y-curve fits, IBM’s model is more conservative when extrapolating from low-weight data, which leads to large overestimates of the logical error rate.

The low accuracy comes from how the two models handle fault-tolerance information. In IBM’s model, the fault-tolerant threshold  $t = \frac{d-1}{2}$  is not encoded explicitly, so the extrapolation toward the fault-tolerant subspaces is intentionally conservative. In contrast, our S-curve model hard-codes  $t = \frac{d-1}{2}$  and constrains the fitted Y-curve to diverge as  $w \rightarrow t^+$ . These results suggest that explicitly modeling the fault-tolerant threshold substantially increases the accuracy.

**Effectiveness of our model.** Here is a generalization of our S-curve model that takes an additional parameter  $s$ , which is a positive real number:

$$f_t^s[\mu, \alpha, \beta](w) = \begin{cases} \frac{1}{2} \cdot \frac{1}{1 + \exp\left(-\frac{w-\mu}{\alpha} + \frac{\beta}{(w-t)^s}\right)} & \text{when } t < w, \\ 0 & \text{when } w \leq t. \end{cases} \quad (11)$$

When  $s = \frac{1}{2}$ , this is the same S-curve as defined in Definition 3. We will test  $s = \frac{1}{4}, \frac{1}{3}, 1, 2$ .

Table 6 reports the logical error rate estimated by ScaLER under different S-curve variants, along with the relative inaccuracy with respect to Stim. Among the tested setting,  $s = \frac{1}{2}$  yields the highest accuracy.

Figure 13 helps to explain this trend. When  $s$  decreases to  $\frac{1}{4}$ , the corresponding Y-curve increases slowly as it approaches the fault-tolerant region, causing ScaLER to overestimate the LER. In contrast, when  $s = 2$ , the Y-curve rises too sharply, making ScaLER underestimate the LER.

In conclusion, our Y-curve fitting framework is compatible with a broad family of S-curve models. Among the variants we evaluated, our chosen S-curve achieves the highest accuracy.

## 9 Threats to Validity

**Do All QEC-Test data Have S-Curves?** Beverland et al. [19] proved the S-curve behavior based on a specific set of assumptions. However, there is currently still no rigorous mathematical proof from first principles that all QEC-test data have S-curves. For future QEC circuits, new and better models may be needed in different noise models, decoder algorithms, and compilation schemes.

**Elusive Ground Truth.** We use Stim output as ground truth, which works up to distance 10, above which Stim doesn’t scale with a two-hour time budget. For larger distances, the ground truth is elusive, and we gain confidence in the ScaLER output by repeating each experiment and calculating the confidence interval.

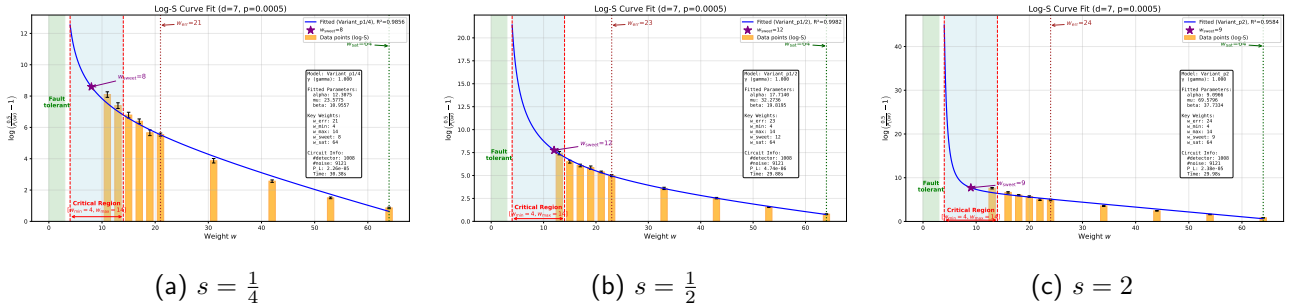


Figure 12: Illustration of Y-curve fitting on the same Surface code  $d = 7$  circuit with  $p = 0.0005$  on different variants of S-curve model. When  $s = \frac{1}{2}$ , the model extrapolate well for the actual data we observe.

Code	d	$s = \frac{1}{4}$		$s = \frac{1}{3}$		$s = \frac{1}{2}$ (Our S-curve model)		$s = 1$		$s = 2$	
		LER	Rel. error vs Stim	LER	Rel. error vs Stim	LER	Rel. error vs Stim	LER	Rel. error vs Stim	LER	Rel. error vs Stim
Surface	3	$9.96 \times 10^{-4}$	72.7%	$9.91 \times 10^{-4}$	71.8%	$5.81 \times 10^{-4}$	0.7%	$1.00 \times 10^{-3}$	74.1%	$1.06 \times 10^{-3}$	83.9%
	5	$1.28 \times 10^{-4}$	99.3%	$1.02 \times 10^{-4}$	58.7%	$3.98 \times 10^{-5}$	-37.9%	$2.87 \times 10^{-5}$	-55.2%	$3.24 \times 10^{-5}$	-49.5%
	7	$2.37 \times 10^{-5}$	299.1%	$1.15 \times 10^{-5}$	93.6%	$3.70 \times 10^{-6}$	-37.8%	$1.37 \times 10^{-6}$	-76.9%	$2.23 \times 10^{-5}$	274.1%
Toric	9	$2.53 \times 10^{-6}$	603.9%	$9.32 \times 10^{-7}$	159.7%	$3.52 \times 10^{-7}$	-1.9%	$6.66 \times 10^{-7}$	85.6%	$1.42 \times 10^{-5}$	3853.8%
	3	$6.38 \times 10^{-4}$	-9.5%	$7.52 \times 10^{-4}$	6.6%	$7.51 \times 10^{-4}$	6.5%	$7.40 \times 10^{-4}$	5.0%	$7.18 \times 10^{-4}$	1.9%
	5	$1.86 \times 10^{-4}$	123.7%	$1.02 \times 10^{-4}$	22.5%	$4.40 \times 10^{-5}$	-47.1%	$5.23 \times 10^{-5}$	-37.1%	$3.49 \times 10^{-5}$	-58.0%
	7	$2.38 \times 10^{-5}$	248.9%	$1.09 \times 10^{-5}$	60.2%	$4.43 \times 10^{-6}$	-35.0%	$2.29 \times 10^{-6}$	-66.4%	$2.51 \times 10^{-5}$	267.9%
	9	$2.52 \times 10^{-6}$	453.1%	$1.39 \times 10^{-6}$	205.0%	$4.23 \times 10^{-7}$	-7.2%	$8.53 \times 10^{-7}$	87.0%	$9.76 \times 10^{-6}$	2039.9%

Table 6: RQ3 (Different S-curve model selection): For each S-curve variant  $f_t^s$  in Eq. 11 with  $s \in \{\frac{1}{4}, \frac{1}{3}, \frac{1}{2}, 1, 2\}$ , we report the estimated LER and the accuracy relative to Stim. When  $s = \frac{1}{2}$ , Stim and ScaLER reach the maximal agreement that we have observed.

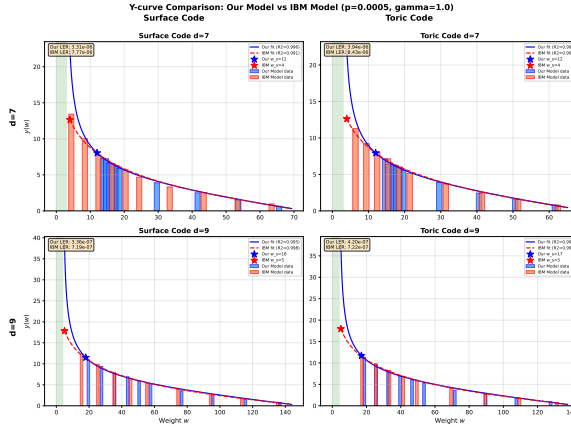


Figure 13: Comparison of fitting and extrapolation between our S-curve model and IBM's S-curve model.

## 10 Related Work

**Stim: the State-of-the-Art Tool.** Stim [13] is a state-of-the-art and widely used tool to simulate QEC based on randomized fault injection. It is highly optimized at the software and system levels, enabling fast circuit simulation. However, Stim scales poorly to large distances. In this paper, we complement Stim by introducing a different approach that scales to large code distances, with a modest time budget.

**Rare-Event Testing of QEC.** Beverland et al. [19] proposed three methods to test error cor-

rection, namely 1) fitting to a failure-spectrum ansatz, 2) a splitting method with metropolis sampling, and 3) multi-seeded splitting. One of their failure-spectrum ansatzes is an S-curve model that appeared earlier in our Definition 2.

Our work goes further by providing an end-to-end algorithm for subspace selection and curve fitting under a fixed time budget. We also give a better S-curve model, an open-source tool, and an experimental comparison with both their failure-spectrum ansatz and with Stim.

Carolyn et al. [22] identify the same challenge and propose addressing the limitations of standard Monte Carlo methods using subset sampling and splitting techniques, similar to the splitting method of Beverland et al. [19].

## Testing heterogeneous QEC architectures.

A growing line of work explores *heterogeneous* fault-tolerant architectures that combine multiple code families. For example, Stein et al. [52] evaluate a heterogeneous architecture that couples surface-code patches with a QLDPC (“gross”) code. Rather than performing an end-to-end fault-injection simulation of the full compiled workload, they use an *instruction-level* error model: they estimate circuit fidelity by *summing* per-operation logical error contributions. This compositional estimator necessar-

Code	d	ScaLER LER (IBM Model)	Rel. error vs Stim	Rel. error factor ( $\times$ )
Surface	3	$1.06 \times 10^{-3}$	83.7%	$119.6 \times$
	5	$9.28 \times 10^{-5}$	44.8%	$1.18 \times$
	7	$9.56 \times 10^{-6}$	60.7%	$1.61 \times$
	9	$7.50 \times 10^{-7}$	109.0%	$54.5 \times$
Toric	3	$5.33 \times 10^{-4}$	-24.4%	$3.75 \times$
	5	$9.51 \times 10^{-5}$	14.3%	$0.30 \times$
	7	$1.16 \times 10^{-5}$	70.0%	$2.00 \times$
	9	$6.76 \times 10^{-7}$	48.1%	$6.68 \times$

Table 7: Comparison of LER estimation of Surface and Toric codes using ScaLER with the IBM S-curve model at  $p = 0.0005$ . The inaccuracy factor is computed as  $|\text{Rel. error}_{\text{IBM vs Stim}}|/|\text{Rel. error}_{\text{Our model vs Stim}}|$ , where  $\text{Rel. error}_{\text{Our model vs Stim}}$  is taken from Table 5.

ily relies on strong assumptions (e.g., independence/locality of logical faults and simplified models for high-weight non-Clifford operators), and it does not capture correlated failure mechanisms arising from code switching, data movement, and scheduling in heterogeneous systems. At the same time, fully detailed end-to-end simulations are often computationally prohibitive for such architectures due to the complexity of compilation/transpilation and cross-code dynamics. We leave to future work to apply our approach to heterogeneous QEC architectures.

**Formal Methods.** Wang et al. [53] developed a symbolic execution approach to testing QEC circuits, followed by a formal verification method using Coq to test circuit fault tolerance [54]. However, in contrast to our paper, these approaches have so far been unable to estimate the logical error rate.

**Fault Injection in Classical Software Testing.** Fault injection is widely used in classical software testing. For example, Feng et al. [55] proposed a coverage-guided fault injection method to evaluate fault recovery in distributed systems. Gao et al. [56] developed an efficient fault injection approach for cloud systems, prioritizing mutation combinations based on runtime feedback. Leveugle et al. [57] provided a method to quantify error and statistical confidence in randomized fault injection. Khanfir [58] explored generative models and bug reports for fault injection. In the spirit of those papers and many more for classical computing, Stim is the best-known tool for fault-injection in quantum computing.

## 11 Future Work

Our approach uses the error model SID, which is a variant of SD6 [23, 9] but different from SI1000 [23]. We leave to future work to enable our approach to take an error model as a parameter.

Our approach uses a hyperparameter  $\Gamma$ , which we use in the definition of the sweet spot. We leave to future work to autotune the value of  $\Gamma$ , which may require a larger time budget than the two hours we use in this paper.

## 12 Conclusion

We have introduced ScaLER, a novel approach and tool to efficiently estimate the logical error rate of QEC circuits. Our experiments reveal a consistent S-curve behavior across all benchmark circuits, which we model with a simple, understandable framework. Our S-curve model captures both the circuit’s fault tolerance and its performance degradation as the number of errors increase. Crucially, the model’s continuity reduces the testing effort required to fit and learn its parameters. ScaLER takes advantage of this insight by integrating model fitting with stratified fault injection, achieving better scalability than Stim.

**Acknowledgments.** We thank Quan Do and Keli Huang for helpful comments on a draft of the article. We are supported by the NSF QLCI program through grant number OMA-2016245 and also by NSF grant number 2422170.

## References

[1] Ben W. Reichardt, Adam Paetznick, David Aasen, Ivan Basov, Juan M. Bello-Rivas, Parsa Bonderson, Rui Chao, Wim van Dam, Matthew B. Hastings, Andres Paz, Marcus P. da Silva, Aarthi Sundaram, Krysta M. Svore, Alexander Vaschillo, Zhenghan Wang, Matt Zanner, William B. Cairncross, Cheng-An Chen, Daniel Crow, Hyosub Kim, Jonathan M. Kindem, Jonathan King, Michael McDonald, Matthew A. Norcia, Albert Ryou, Mark Stone, Laura Wadleigh, Katrina Barnes, Peter Battaglino, Thomas C. Bohdanowicz, Graham Booth, Andrew Brown, Mark O. Brown, Kayleigh Cassella, Robin Coxe, Jeffrey M. Epstein, Max Feldkamp, Christopher Griger, Eli Halperin, Andre Heinz, Frederic Hummel, Matthew Jaffe, Antonia M. W. Jones, Eliot Kapit, Krish Kotru, Joseph Lauigan, Ming Li, Jan Marjanovic, Eli Megidish, Matthew Meredith, Ryan Morshead, Juan A. Muniz, Sandeep Narayanaswami, Ciro Nishiguchi, Timothy Paule, Kelly A. Pawlak, Kristen L. Pudenz, David Rodríguez Pérez, Jon Simon, Aaron Smull, Daniel Stack, Miroslav Urbanek, René J. M. van de Veerdonk, Zachary Vendeiro, Robert T. Weverka, Thomas Wilkason, Tsung-Yao Wu, Xin Xie, Evan Zalys-Geller, Xiaogang Zhang, and Benjamin J. Bloom. “Logical computation demonstrated with a neutral atom quantum processor” (2024). [arXiv:2411.11822](https://arxiv.org/abs/2411.11822).

[2] Sergey Bravyi, Andrew W. Cross, Jay M. Gambetta, Dmitri Maslov, Patrick Rall, and Theodore J. Yoder. “High-threshold and low-overhead fault-tolerant quantum memory”. *Nature* **627**, 778–782 (2024).

[3] Pedro Sales Rodriguez, John M. Robinson, Paul Niklas Jepsen, Zhiyang He, Casey Duckering, Chen Zhao, Kai-Hsin Wu, Joseph Campo, Kevin Bagnall, Minho Kwon, Thomas Karolyshyn, Phillip Weinberg, Madelyn Cain, Simon J. Evered, Alexandra A. Geim, Marcin Kalinowski, Sophie H. Li, Tom Manovitz, Jesse Amato-Grill, James I. Basham, Liane Bernstein, Boris Braverman, Alexei Bylinskii, Adam Choukri, Robert DeAngelo, Fang Fang, Connor Fieweger, Paige Frederick, David Haines, Majd Hamdan, Julian Hammett, Ning Hsu, Ming-Guang Hu, Florian Huber, Ningyuan Jia, Dhruv Kedar, Milan Kornjača, Fangli Liu, John Long, Jonathan Lopatin, Pedro L. S. Lopes, Xiu-Zhe Luo, Tommaso Macrì, Ognjen Marković, Luis A. Martínez-Martínez, Xianmei Meng, Stefan Ostermann, Evgeny Ostroumov, David Paquette, Zexuan Qiang, Vadim Shofman, Anshuman Singh, Manuj Singh, Nandan Sinha, Henry Thoreen, Noel Wan, Yiping Wang, Daniel Waxman-Lenz, Tak Wong, Jonathan Wurtz, Andrii Zhdanov, Laurent Zheng, Markus Greiner, Alexander Keesling, Nathan Gemelke, Vlada Vuletić, Takuya Kitagawa, Sheng-Tao Wang, Dolev Bluvstein, Mikhail D. Lukin, Alexander Lukin, Hengyun Zhou, and Sergio H. Cantú. “Experimental demonstration of logical magic state distillation” (2024). [arXiv:2412.15165](https://arxiv.org/abs/2412.15165).

[4] Rajeev Acharya, Dmitry A Abanin, Laleh Aghababaie-Beni, Igor Aleiner, Trond I Andersen, Markus Ansmann, Frank Arute, Kunal Arya, Abraham Asfaw, Nikita Asatrkhantsev, et al. “Quantum error correction below the surface code threshold”. *Nature* (2024).

[5] Peter W Shor. “Polynomial-time algorithms for prime factorization and discrete logarithms on a quantum computer”. *SIAM review* **41**, 303–332 (1999).

[6] Aram W. Harrow, Avinatan Hassidim, and Seth Lloyd. “Quantum algorithm for linear systems of equations”. *Physical Review Letters* **103** (2009).

[7] Lov K. Grover. “A fast quantum mechanical algorithm for database search” (1996). [arXiv:quant-ph/9605043](https://arxiv.org/abs/quant-ph/9605043).

[8] A. Paetznick, M. P. da Silva, C. Ryan-Anderson, J. M. Bello-Rivas, J. P. Campora III, A. Chernoguzov, J. M. Dreiling, C. Foltz, F. Frachon, J. P. Gaebler, T. M. Gatterman, L. Grans-Samuelsson, D. Gresh, D. Hayes, N. Hewitt, C. Holliman, C. V. Horst, J. Johansen, D. Lucchetti, Y. Matsuoka, M. Mills, S. A. Moses, B. Neyenhuis, A. Paz, J. Pino, P. Siegfried, A. Sundaram, D. Tom, S. J. Wernli, M. Zanner, R. P. Stutz, and K. M. Svore. “Demonstration of logical qubits and repeated er-

ror correction with better-than-physical error rates" (2024). [arXiv:2404.02280](https://arxiv.org/abs/2404.02280).

[9] György P Gehér, Campbell McLauchlan, Earl T Campbell, Alexandra E Moylett, and Ophelia Crawford. "Error-corrected hadamard gate simulated at the circuit level". *Quantum* **8**, 1394 (2024).

[10] Anbang Wu, Gushu Li, Hezi Zhang, Gian Giacomo Guerreschi, Yufei Ding, and Yuan Xie. "A synthesis framework for stitching surface code with superconducting quantum devices". In Proceedings of the 49th Annual International Symposium on Computer Architecture. [Page 337–350](#). ISCA '22 New York, NY, USA (2022). Association for Computing Machinery.

[11] Bálint Domokos, Áron Márton, and János K. Asbóth. "Characterization of errors in a CNOT between surface code patches". *Quantum* **8**, 1577 (2024).

[12] Yu Tomita and Krysta M. Svore. "Low-distance surface codes under realistic quantum noise". *Physical Review A* **90** (2014).

[13] Craig Gidney. "Stim: a fast stabilizer circuit simulator". *Quantum* **5**, 497 (2021).

[14] Craig Gidney, Michael Newman, and Matt McEwen. "Benchmarking the planar honeycomb code". *Quantum* **6**, 813 (2022).

[15] Tom Peham, Ludwig Schmid, Lucas Berent, Markus Müller, and Robert Wille. "Automated synthesis of fault-tolerant state preparation circuits for quantum error-correction codes". *PRX Quantum* **6**, 020330 (2025).

[16] Craig Gidney, Michael Newman, Peter Brooks, and Cody Jones. "Yoked surface codes" (2023). [arXiv:2312.04522](https://arxiv.org/abs/2312.04522).

[17] Craig Gidney. "A Pair Measurement Surface Code on Pentagons". *Quantum* **7**, 1156 (2023).

[18] Sascha Heußen, Don Winter, Manuel Rispler, and Markus Müller. "Dynamical subset sampling of quantum error-correcting protocols". *Physical Review Research* **6** (2024).

[19] Michael E. Beverland, Malcolm Carroll, Andrew W. Cross, and Theodore J. Yoder. "Fail fast: techniques to probe rare events in quantum error correction" (2025). [arXiv:2511.15177](https://arxiv.org/abs/2511.15177).

[20] Mei-Chen Hsueh, T.K. Tsai, and R.K. Iyer. "Fault injection techniques and tools". *Computer* **30**, 75–82 (1997).

[21] Craig Gidney and Martin Ekerå. "How to factor 2048 bit RSA integers in 8 hours using 20 million noisy qubits". *Quantum* **5**, 433 (2021).

[22] Carolyn Mayer, Anand Ganti, Uzoma Onunkwo, Tzvetan Metodi, Benjamin Anker, and Jacek Skryzalin. "Rare event simulation of quantum error-correcting circuits" (2025). [arXiv:2509.13678](https://arxiv.org/abs/2509.13678).

[23] Craig Gidney, Michael Newman, Austin Fowler, and Michael Broughton. "A Fault-Tolerant Honeycomb Memory". *Quantum* **5**, 605 (2021).

[24] Dorit Aharonov, Alexei Kitaev, and John Preskill. "Fault-tolerant quantum computation with long-range correlated noise". *Physical review letters* **96**, 050504 (2006).

[25] Rajeev Acharya, Igor Aleiner, Richard Allen, Trond I. Andersen, Markus Ansmann, Frank Arute, Kunal Arya, Abraham Asfaw, Juan Atalaya, Ryan Babbush, Dave Bacon, Joseph C. Bardin, Joao Basso, Andreas Bengtsson, Sergio Boixo, Gina Bortoli, Alexandre Bourassa, Jenna Bovaird, Leon Brill, Michael Broughton, Bob B. Buckley, David A. Buell, Tim Burger, Brian Burkett, Nicholas Bushnell, Yu Chen, Zijun Chen, Ben Chiaro, Josh Cogan, Roberto Collins, Paul Conner, William Courtney, Alexander L. Crook, Ben Curtin, Dripto M. Debroy, Alexander Del Toro Barba, Sean Demura, Andrew Dunsworth, Daniel Eppens, Catherine Erickson, Lara Faoro, Edward Farhi, Reza Fatemi, Leslie Flores Burgos, Ebrahim Forati, Austin G. Fowler, Brooks Foxen, William Giang, Craig Gidney, Dar Gilboa, Marissa Giustina, Alejandro Grajales Dau, Jonathan A. Gross, Steve Habegger, Michael C. Hamilton, Matthew P. Harrigan, Sean D. Harrington, Oscar Higgott, Jeremy Hilton, Markus Hoffmann, Sabrina Hong, Trent Huang, Ashley Huff, William J. Huggins, Lev B. Ioffe, Sergei V. Isakov, Justin Iveland, Evan Jeffrey, Zhang Jiang, Cody Jones, Pavol Juhas, Dvir Kafri,

Kostyantyn Kechedzhi, Julian Kelly, Tanuj Khattar, Mostafa Khezri, Mária Kieferová, Seon Kim, Alexei Kitaev, Paul V. Klimov, Andrey R. Klots, Alexander N. Korotkov, Fedor Kostritsa, John Mark Kreikebaum, David Landhuis, Pavel Laptev, Kim-Ming Lau, Lily Laws, Joonho Lee, Kenny Lee, Brian J. Lester, Alexander Lill, Wayne Liu, Aditya Locharla, Erik Lucero, Fionn D. Malone, Jeffrey Marshall, Orion Martin, Jarrod R. McClean, Trevor McCourt, Matt McEwen, Anthony Megrant, Bernardo Meurer Costa, Xiao Mi, Kevin C. Miao, Masoud Mohseni, Shirin Montazéri, Alexis Morvan, Emily Mount, Wojciech Mruczkiewicz, Ofer Naaman, Matthew Neeley, Charles Neill, Ani Nersisyan, Hartmut Neven, Michael Newman, Jiun How Ng, Anthony Nguyen, Murray Nguyen, Murphy Yuezhen Niu, Thomas E. O'Brien, Alex Opremcak, John Platt, Andre Petukhov, Rebecca Potter, Leonid P. Pryadko, Chris Quintana, Pedram Roushan, Nicholas C. Rubin, Negar Saei, Daniel Sank, Kannan Sankaragomathi, Kevin J. Satzinger, Henry F. Schurkus, Christopher Schuster, Michael J. Shearn, Aaron Shorter, Vladimir Shvarts, Jindra Skruzny, Vadim Smelyanskiy, W. Clarke Smith, George Sterling, Doug Strain, Marco Szalay, Alfredo Torres, Guifre Vidal, Benjamin Villalonga, Catherine Vollgraff Heidweiller, Theodore White, Cheng Xing, Z. Jamie Yao, Ping Yeh, Juhwan Yoo, Grayson Young, Adam Zalcman, Yaxing Zhang, and Ningfeng Zhu. “Suppressing quantum errors by scaling a surface code logical qubit”. *Nature* **614**, 676–681 (2023).

[26] Daniel Gottesman. “Theory of fault-tolerant quantum computation”. *Physical Review A* **57**, 127 (1998).

[27] Peter W. Shor. “Fault-tolerant quantum computation”. In *Proceedings of the 37th Annual Symposium on Foundations of Computer Science (FOCS)*. Pages 56–65. IEEE (1996).

[28] Seok-Hyung Lee, Andrew Li, and Stephen D. Bartlett. “Color code decoder with improved scaling for correcting circuit-level noise”. *Quantum* **9**, 1609 (2025).

[29] Jun Han and Claudio Moraga. “The influence of the sigmoid function parameters on the speed of backpropagation learning”. In *International workshop on artificial neural networks*. Pages 195–201. Springer (1995).

[30] George Cybenko. “Approximation by superpositions of a sigmoidal function”. *Mathematics of control, signals and systems* **2**, 303–314 (1989).

[31] Xinyou Yin, JAN Goudriaan, Egbert A Lantinga, JAN Vos, and Huub J Spiertz. “A flexible sigmoid function of determinate growth”. *Annals of botany* **91**, 361–371 (2003).

[32] MP Hassell, JH Lawton, and JR Beddington. “Sigmoid functional responses by invertebrate predators and parasitoids”. *The Journal of Animal Ecology* Pages 249–262 (1977).

[33] Marc Klimstra and E Paul Zehr. “A sigmoid function is the best fit for the ascending limb of the hoffmann reflex recruitment curve”. *Experimental brain research* **186**, 93–105 (2008).

[34] Taghi M Khoshgoftaar and Robert M Szabo. “Using neural networks to predict software faults during testing”. *IEEE Transactions on Reliability* **45**, 456–462 (1996).

[35] Javaid Iqbal, Tabasum Firdous, Avinash K Shrivastava, and Iqra Saraf. “Modelling and predicting software vulnerabilities using a sigmoid function”. *International Journal of Information Technology* **14**, 649–655 (2022).

[36] Boost C++ Libraries. “Boost c++ libraries - dynamic\_bitset”. [https://www.boost.org/doc/libs/1\\_36\\_0/libs/dynamic\\_bitset/dynamic\\_bitset.html](https://www.boost.org/doc/libs/1_36_0/libs/dynamic_bitset/dynamic_bitset.html) (2008). Accessed: 2025-07-08.

[37] Leonardo Dagum and Ramesh Menon. “Openmp: an industry standard api for shared-memory programming”. *Computational Science & Engineering, IEEE* **5**, 46–55 (1998).

[38] pybind11 Developers. “pybind11 documentation”. <https://pybind11.readthedocs.io/en/stable/> (2025). Accessed: 2025-07-08.

[39] Pauli Virtanen, Ralf Gommers, Travis E. Oliphant, Matt Haberland, Tyler Reddy, David Cournapeau, Evgeni Burovski, Pearu Peterson, Warren Weckesser, Jonathan Bright, Stéfan J. van der Walt, Matthew Brett, Joshua Wilson, K. Jarrod Millman, Nikolay Mayorov, Andrew R. J. Nelson, Eric Jones, Robert Kern, Eric Larson, C J Carey, İlhan Polat, Yu Feng, Eric W. Moore, Jake VanderPlas, Denis Laxalde, Josef Perktold, Robert Cimrman, Ian Henriksen, E. A. Quintero, Charles R. Harris, Anne M. Archibald, Antônio H. Ribeiro, Fabian Pedregosa, Paul van Mulbregt, and SciPy 1.0 Contributors. “SciPy 1.0: Fundamental Algorithms for Scientific Computing in Python”. *Nature Methods* **17**, 261–272 (2020).

[40] Sergey Bravyi, Andrew W Cross, Jay M Gambetta, Dmitri Maslov, Patrick Rall, and Theodore J Yoder. “High-threshold and low-overhead fault-tolerant quantum memory”. *Nature* **627**, 778–782 (2024).

[41] Michael A. Perlin. “qLDPC”. <https://github.com/qLDPCOrg/qLDPC> (2023).

[42] Oscar Higgott and Craig Gidney. “Sparse blossom: correcting a million errors per core second with minimum-weight matching” (2023).

[43] Joschka Roffe, David R. White, Simon Burton, and Earl Campbell. “Decoding across the quantum low-density parity-check code landscape”. *Physical Review Research* **2** (2020).

[44] Christopher J Ballance, Thomas P Harty, Norbert M Linke, Martin A Sepiol, and David M Lucas. “High-fidelity quantum logic gates using trapped-ion hyperfine qubits”. *Physical review letters* **117**, 060504 (2016).

[45] Wister Huang, CH Yang, KW Chan, T Tanttu, B Hensen, RCC Leon, MA Fogarty, JCC Hwang, FE Hudson, Kohei M Itoh, et al. “Fidelity benchmarks for two-qubit gates in silicon”. *Nature* **569**, 532–536 (2019).

[46] MA Rol, F Battistel, FK Malinowski, CC Bultink, BM Tarasinski, R Vollmer, N Haider, N Muthusubramanian, A Bruno, BM Terhal, et al. “Fast, high-fidelity conditional-phase gate exploiting leakage interference in weakly anharmonic superconducting qubits”. *Physical review letters* **123**, 120502 (2019).

[47] Petar Jurcevic, Ali Javadi-Abhari, Lev S Bishop, Isaac Lauer, Daniela F Bogorin, Markus Brink, Lauren Capelluto, Oktay Günlük, Toshinari Itoko, Naoki Kanazawa, et al. “Demonstration of quantum volume 64 on a superconducting quantum computing system”. *Quantum Science and Technology* **6**, 025020 (2021).

[48] Brooks Foxen, Charles Neill, Andrew Dunsworth, Pedram Roushan, Ben Chiaro, Anthony Megrant, Julian Kelly, Zijun Chen, Kevin Satzinger, Rami Barends, et al. “Demonstrating a continuous set of two-qubit gates for near-term quantum algorithms”. *Physical Review Letters* **125**, 120504 (2020).

[49] Yulin Wu, Wan-Su Bao, Sirui Cao, Fusheng Chen, Ming-Cheng Chen, Xiawei Chen, Tung-Hsun Chung, Hui Deng, Yajie Du, Daojin Fan, et al. “Strong quantum computational advantage using a superconducting quantum processor”. *Physical review letters* **127**, 180501 (2021).

[50] Larry Wasserman. “All of statistics: a concise course in statistical inference”. Springer Science & Business Media. (2004).

[51] Craig Gidney. “How to factor 2048 bit rsa integers with less than a million noisy qubits” (2025). [arXiv:2505.15917](https://arxiv.org/abs/2505.15917).

[52] Samuel Stein, Shifan Xu, Andrew W. Cross, Theodore J. Yoder, Ali Javadi-Abhari, Chenxu Liu, Kun Liu, Zeyuan Zhou, Charlie Guinn, Yufei Ding, Yongshan Ding, and Ang Li. “Hetec: Architectures for heterogeneous quantum error correction codes”. In *Proceedings of the 30th ACM International Conference on Architectural Support for Programming Languages and Operating Systems, Volume 2*. Page 515–528. ASPLOS ’25New York, NY, USA (2025). Association for Computing Machinery.

[53] Wang Fang and Mingsheng Ying. “Symbolic execution for quantum error correction programs”. *Proc. ACM Program. Lang.* **8** (2024).

- [54] Qifan Huang, Li Zhou, Wang Fang, Mengyu Zhao, and Mingsheng Ying. “Efficient formal verification of quantum error correcting programs” (2025).
- [55] Wenhao Feng, Qiugen Pei, Yu Gao, Dong Wang, Wensheng Dou, Jun Wei, Zheheng Liang, and Zhenyue Long. “Faultfuzz: A coverage guided fault injection tool for distributed systems”. In Proceedings of the 2024 IEEE/ACM 46th International Conference on Software Engineering: Companion Proceedings. [Page 129–133](#). ICSE-Companion ’24New York, NY, USA (2024). Association for Computing Machinery.
- [56] Yu Gao, Wensheng Dou, Dong Wang, Wenhao Feng, Jun Wei, Hua Zhong, and Tao Huang. “Coverage guided fault injection for cloud systems”. In Proceedings of the 45th International Conference on Software Engineering. [Page 2211–2223](#). ICSE ’23. IEEE Press (2023).
- [57] Régis Leveugle, A Calvez, Paolo Maistri, and Pierre Vanhauwaert. “Statistical fault injection: Quantified error and confidence”. In 2009 Design, Automation & Test in Europe Conference & Exhibition. Pages 502–506. IEEE (2009).
- [58] Ahmed Khanfir. “Effective and scalable fault injection using bug reports and generative language models”. In Proceedings of the 30th ACM Joint European Software Engineering Conference and Symposium on the Foundations of Software Engineering. [Page 1790–1794](#). ESEC/FSE 2022New York, NY, USA (2022). Association for Computing Machinery.